J Solid State Electrochem (2006) 10: 447–457
DOI 10.1007/s10008-005-0034-6

ORIGINAL PAPER

Dijana Šimkūnaitė · Emilija Ivaškevič
Aleksandras Kaliničenko · Antanas Steponavičius

Nucleation and growth of Cu onto polycrystalline Pt electrode from acidic $CuSO_4$ solution in the presence of H_2SeO_3

Received: 25 November 2004 / Revised: 01 June 2005 / Accepted: 09 June 2005 / Published online: 26 July 2005

Abstract The early stages of Cu electrodeposition onto Pt(poly) have been investigated in 0.5 M H_2SO_4 + 0.01 M $CuSO_4$ solution without or with H_2SeO_3 when a molar concentration ratio [Cu(II)]/[Se(IV)] ≥ 2×10^2 using electrochemical and ex situ AFM techniques. The overpotential deposition of Cu has been performed onto a Pt surface precovered independently with Cu in amount close to an equivalent monolayer. Chronoamperometric results have been shown to follow an instantaneous 3D nucleation and diffusion-controlled growth model. The values of diffusion coefficient D for Cu^{2+}, number of nuclei N and average nuclei radius r_{av} have been calculated. In the local regions of the surface, the separate large agglomerates composed of the different diameter clusters have been revealed in both cases, but, in the presence of the H_2SeO_3, they attained a distinct chain-like configuration. Some morphological characteristics have been reported.

Keywords First stages of electrodeposition · Copper · Sulphate solution · H_2SeO_3

Introduction

Nucleation and growth are very important stages in metal electrodeposition process. On the one hand, the competition between growth and nucleation determines the granularity of a metal deposit. On the other hand, the general appearance and structure of a metal deposit are determined by a form of the growing crystals [1].

D. Šimkūnaitė (✉) · E. Ivaškevič · A. Kaliničenko
A. Steponavičius
Institute of Chemistry, Goštauto 9,
LT-01108, Vilnius, Lithuania
E-mail: nemezius@ktl.mii.lt
Tel.: +370-5-2649773
Fax: +370-5-2617067

The early stages of the formation of a new phase onto a foreign substrate are commonly accepted to involve not only a 3D nucleation and growth process, but also adsorption reactions and formation of low-dimensional systems, which are preferentially localized at surface inhomogeneities of a substrate [1, 2].

Copper is probably the most studied metal in electrodeposition because of its industrial importance and great suitability for investigation of the kinetics and mechanism of the electrocrystallization process, including a transition from a 2D sub- or monolayer to a bulk metal deposit [3]. In particular, as early as in the 1970s, it has been shown that the 3D Cu nucleation and growth process onto a polycrystalline Pt (Pt(poly)) substrate at potentials more negative than a reversible potential (E_r) of a Cu^{2+}/Cu redox couple involves a 2D to 3D rearrangement at growing sites [4–7]. Therefore, it has been supposed that, during a certain initial period of electrodeposition, an area of a free Pt(poly) substrate and the 2D Cu domains might coexist with the 3D Cu nuclei [3, 4].

A role of small amounts of various additives in depositing Cu overlayers has already been studied extensively. Particularly, an effect of additives on the early stages of Cu deposition onto a foreign substrate has attracted much attention as well [8–17]. In this context, Se(IV) compounds continue to be of considerable research interest and are being explored for a variety of applications, including electrocatalysis [18–21], electrodeposition of thin layers of copper selenides as semiconduting materials (see, e.g. [20–25]) and as additives showing an accelerating action on the Cu^{2+} discharge at Cu electrode in acidic $CuSO_4$ solutions [26–28].

While the codeposition of Cu and Se onto various substrates and the formation of thin layers of copper selenides have been investigated extensively [20–25], both the discharge of Cu^{2+} ions and the electrocrystallization of Cu under an action of Se(IV) compounds have been studied to a lesser extent. It has been known that much less amounts of these compounds, namely,

ranging from 10^{-6} to 10^{-4} M, and at a molar concentration ratio [Cu(II)]/[Se(IV)] from 10^3 to 10^5, are typically used when the discharge reaction of Cu^{2+} itself is to be studied, as compared with the electrodeposition of copper selenides, when comparable amounts of Cu(II) and Se(IV) have commonly been applied. Moreover, the acceleration phenomenon has principally been studied in a region of lower values of overpotentials [26–28]. The early stages of Cu deposition onto a foreign substrate in the presence of Se(IV) compounds are also less understood. As far as we know, there are only several studies in the system Cu + Se, for example, onto Se-precovered Au(poly) [29] and Pt(poly) [30, 31] electrodes. However, no efforts focused on the investigation of the early stages of Cu deposition onto a foreign substrate in the presence of dissolved Se(IV) compounds have been found.

Herein, we present an electrochemical study and AFM analysis performed on a Pt(poly) surface in the early stages of Cu deposition process from an acidic $CuSO_4$ solution containing H_2SeO_3. Attention was also given to the Cu underpotential deposition (UPD) onto a Pt(poly) surface in the presence of this additive in order to characterize a surface state of Pt prior to the subsequent electrochemical or structural measurements.

Experimental

The working solution was 0.5 M H_2SO_4 + 0.01 M $CuSO_4$ containing H_2SeO_3 in amounts of 1×10^{-3} to 5×10^{-2} mM. The molar concentration ratio [Cu(II)]/[Se(IV)] was no less than 2×10^2 . The electrolytes were prepared from doubly distilled water, copper sulphate (Fluka) preheated at 400°C for 4 h, highest purity sulphuric acid (Russia) and selenious acid (99.999% purity, Aldrich). Prior to each experiment, the working solution was deaerated with Ar gas for 0.5 h.

All experiments were carried out at 20 ± 0.1°C in a conventional three-electrode cell. The working electrode was a vertical disc with a diameter of 10.5 mm made from a polycrystalline Pt foil (99.99% purity, Russia). The counter electrode was a Pt sheet of ca. 4 cm^2 in area, and the reference electrode was a Ag/AgCl/KCl(sat.) electrode. In the text, all potentials (*E*s) were recalculated with respect to the standard hydrogen electrode (SHE), unless otherwise stated.

The real surface area of the Pt(poly) electrode was determined from a hydrogen adsorption current-potential profile recorded at 50 mVs^{-1} in 0.5 M H_2SO_4 solution, taking a specific charge of 210 μC cm^{-2} for the complete coverage of Pt(poly) by adsorbed hydrogen, as reported in [32]. The roughness factor (*f*) was obtained to be 2.05 ± 0.05. All currents in the text are presented as current densities with respect to the visible surface area of the Pt electrode.

The pretreatment of the Pt(poly) electrode prior to the electrochemical measurements was described elsewhere [31, 33]. The electrochemical investigations were carried out using cyclic voltammetry and single potential step techniques, as mentioned above. In all cases, the Pt(poly) electrode was first allowed to stand at a starting potential (E_{start}) for 2 min. The value of E_{start} was varied depending on a method applied: (a) the potential sweeps were started with E_{start} = +0.85 V, at first, towards more negative *E*s; (b) the potentiostatic cathodic current-time transients (*I*/*t*) were recorded starting with E_{start} = +0.35 V or, in some instances, with +0.80 V. The reasons for choosing such values of E_{start} are presented below. The cyclic voltammograms (CVs) and potentiostatic *I*/*t* curves were recorded using a PI 50-1 potentiostat (Belarus) interfaced through a home-made analogue to digital converter with a PC (Siemens) and a PR-8 programmer (Belarus).

The samples for the ex situ AFM investigations were prepared in such a way that (1) the working Pt(poly) electrode after the pretreatment, as described in [31, 33], was allowed to stand at *E* = +0.35 V, analogously to the case of the chronoamperometric measurements; (2) as in (1) followed by a single potential pulse to E_{dep} = +0.23 V located in the region of Cu overpotentials for 10 or 30 s. It was found that an image captured at a given time of applied E_{dep} was reproducible. The AFM observation was performed using a TopoMetrix Explorer SPM with a Si_3N_4 tip operating in a contact mode. The top-view images are presented in so-called "height mode" where the higher parts appear brighter. A cross-sectional analysis of an AFM image was also applied.

The Nernst potential (E_r) for a couple Cu^{2+}/Cu was estimated by measuring an open-circuit potential (OCP) of bulk Cu in unstirred 0.5 M H_2SO_4 + 0.01 M $CuSO_4$ solution at 20°C and was found to be equal to +0.260 V.

Results and discussion

Cu deposition in the region of underpotentials

The results of cyclic voltammetry, chronoamperometry and also of AFM imaging obtained with the working Pt(poly) electrode in the region of Cu underpotentials were used to characterize the surface of this electrode prior to the investigation of the early stages of Cu overpotential deposition (OPD) as mentioned above.

Figure 1 shows the Cu UPD voltammetric responses in 0.5 M H_2SO_4 + 0.01 M $CuSO_4$ solution containing increasing amounts of H_2SeO_3. The CVs were recorded in such range of potentials (*E*s) where a contribution of Pt(poly) substrate oxidation and reduction of surface platinum oxide to Cu UPD/stripping reactions can be ruled out. In particular, in 0.5 M H_2SO_4 solution, which is of interest herein, the platinum oxide formation starts at +0.85 V [34].

The cyclic voltammetry of the Cu UPD onto Pt(poly) is well documented in the literature (see, e.g. [4, 7, 33, 35]) and, therefore, there is no need to go into details of

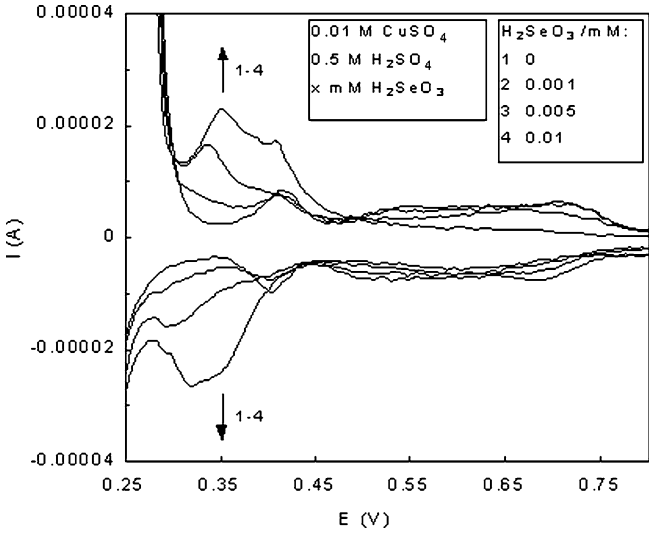

Fig. 1 Typical CVs (the first sweep) for Pt(poly) electrode in 0.5 M H_2SO_4 + 0.01 M $CuSO_4$ solution containing increasing amounts of H_2SeO_3. The sweeps were carried out between $E_{s,a} = +0.85$ V and $E_{s,c} = +0.25$ V at a sweep rate $v = 2$ mV s^{-1}

analysing the curves presented here. It is sufficient to point that the overall shape of the CV recorded in the absence of H_2SeO_3 is the same as that described in other studies of the Cu UPD onto bare Pt(poly) in acidic $CuSO_4$ solutions [7, 33, 35]. The addition of H_2SeO_3 resulted in a change of this profile. A specific voltammetric pattern of this process disappeared, and a complex current peak moved in the cathodic direction to potentials close to the E_r (curves 2–5). It is noteworthy that rather good parallelism is observed between the CVs (Fig. 1) and those obtained for a Se-modified Pt(poly) electrode in pure acidic $CuSO_4$ solution [33], indicating, therefore, that in either case the Cu UPD process seems to take place at Pt substrates of similar surface properties. From the results of voltammetric and XPS investigations [33, 36, 37], it has been concluded that the coadsorption of Cu and Se species may occur onto a Pt(poly) surface. Then, one can expect two layer structures to be possible: either the segregated layers of Cu and Se or the mixed layers of these elements. The discrimination between these possible layer structures at present appears to be rather difficult. In relation to this problem, it is pertinent to note that a certain amount of metallic Cu, less than one monolayer deposited underpotentially onto Pt(poly), and the presence of zero valence Se species in amounts not exceeding a few at. % have been identified by means of XPS after exposure of Pt(poly) at +0.35 V to H_2SO_4 + $CuSO_4$ solution with H_2SeO_3 at the same values of molar concentration ratio [Cu(II)]/[Se(IV)] [36, 37].

The voltammetric results (Fig. 1) suggest that, in the presence of even low amounts of H_2SeO_3 in the working solution, for example at the molar concentration ratio of 2×10^3, the Cu UPD onto Pt(poly) is inhibited by, most likely, adsorbed Se species. At this stage, an attempt to explain this experimental result is rather speculative. One such reason may be that, even though the surface amount of Se is quite small, the specifically adsorbed Se species are capable to show a long-range effect upon the electronic properties of the Pt(poly) substrate.

In order to get more information on the surface state of the working Pt(poly) electrode before studying the early stages of Cu deposition, the potential step within the Cu UPD range and AFM techniques were further applied.

Figure 2 shows a series of typical potentiostatic current transients recorded in the working solution without or with H_2SeO_3 starting with $E_{start} = +0.8$ V to various E_{dep} located in the Cu UPD region, as mentioned above. Such value of E_{start} was chosen because no evidence pointed to the occurrence of Cu UPD at this E has been found (see, e.g. [5, 7]). The potential step from this E_{start}, therefore, was thought to be performed with a Cu-uncovered Pt(poly) electrode.

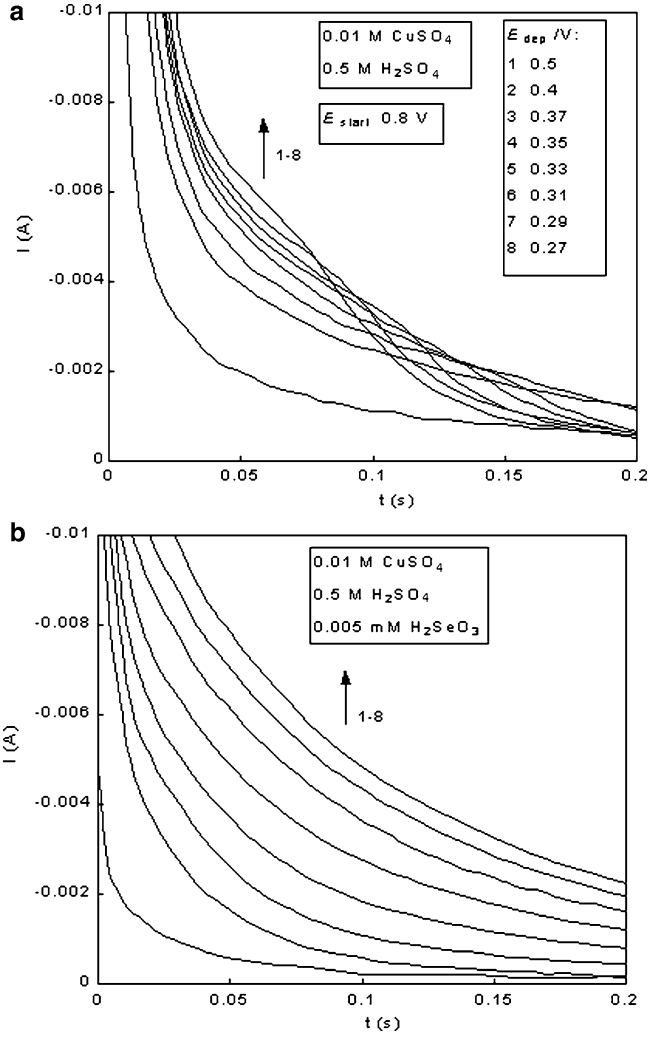

Fig. 2 Typical potentiostatic current transients for the Cu UPD onto Pt(poly) recorded by stepping from $E_{start} = +0.80$ V to various E_{dep} in the UPD region in 0.5 M H_2SO_4 + 0.01 M $CuSO_4$ solution without (**a**) or with 0.005 mM H_2SeO_3 (**b**)

Monotonically decreasing current transients were registered in the H_2SeO_3-free solution in the E_{dep} region from +0.50 to about +0.35 V (Fig. 2a) implying an adsorption process to be dominant [38] (the transients at E_{dep} +0.70 and +0.60 V are not shown). At more negative E_{dep}, the initial current decrease is followed by a shoulder-like region, which should be typical of the adsorption coupled with 2D nucleation/growth [38]. In the presence of H_2SeO_3, only monotonic current transients were obtained (Fig. 2b), suggesting the dominant role of adsorption.

Integration of the current transients recorded by stepping from +0.80 V to a certain value of E_{dep}, say, +0.35 V, yielded the reduction charges of about 440 and 400 μC cm^{-2} in the absence and in the presence of H_2SeO_3 (Fig. 3). These values of charge density give about 1 or 0.9 equivalent monolayer of Cu, respectively. Somewhat overestimated values of monolayer charge density at $E_{dep} < +0.35$ V in pure $CuSO_4$ solution are likely attributed to more than one complete monolayer of Cu adatoms and also to the coexistence of some amount of 2D phase, as supposed in [7, 39].

AFM images (Fig. 4a) confirmed that, at $E_{dep} = +0.35$ V, the Cu UPD process involves not only the deposition of the randomly adsorbed Cu layer, but the additional formation of more ordered structures of the Cu species in some local regions as well, especially at the Pt(poly) electrode surface defects acting as the most active sites for this process. In the H_2SeO_3-free solution the individual Cu species are of comparatively uniform size (Figs. 4a, 5a). Moreover, the Cu deposition seems to be uneven along such surface defects, as polishing scratches, because some rather sharp protrusions were also resolved. From the standard roughness measurements (Fig. 5a) it can be seen that the arithmetic average of the absolute values of measured profile height deviations (with the number of height positions along each line profiles equal to 5 in 5 μm × 5 μm section), that is, arithmetic roughness average, R_a, was on the average 6.9 nm, and the maximum height of the profiles above the mean lines, R_p, was on the average 43.9 nm. These measurements clearly show the rather significant contribution of the separate large protrusions into the overall surface roughness.

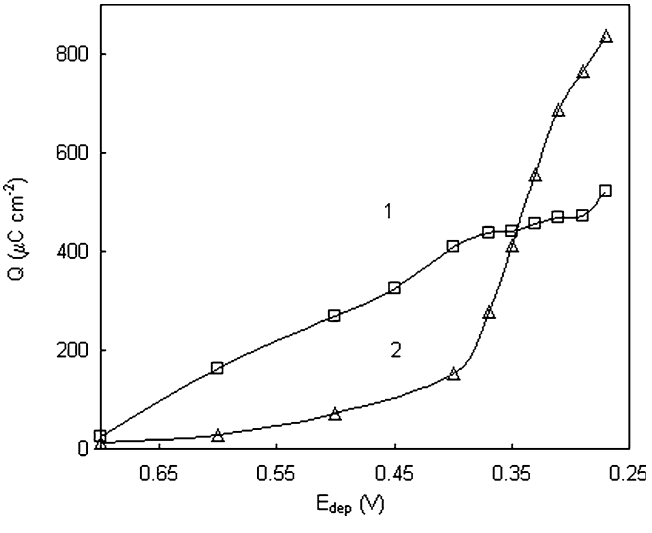

Fig. 3 Variation of cathodic charge densities with deposition potential E_{dep} in the absence (*1*) and in the presence of H_2SeO_3 (*2*) (from current transients in Fig. 2)

In principle, the situation remains similar when the Cu UPD takes place in the presence of H_2SeO_3 (Figs. 4b and 5b). The main difference is that the distinct chain-like structures are present on the surface. These structures were found to be composed of numerous separate spherical particles. In the presence of H_2SeO_3, the surface of the specimen was somewhat more rough, as reflected in its surface roughness characteristics, in particular, R_a was on the average 7.6 nm and R_p 38.2 nm (Fig. 5b).

The main points that can be extracted to characterize a state of the substrate surface before the potential excursion into the Cu OPD zone from the experimental data presented here and from those reported in the literature [7, 31, 33, 35–37, 39] seem to be as follows.

1. The integral information from the entire Pt(poly) surface by the conventional electrochemical measuring techniques is sufficient to reason that the *E* pulse into the region of Cu overpotentials will be performed with the Pt(poly) surface precovered independently with Cu (Cu_{UPD}), and, as a result, the Cu OPD involves Cu deposition onto the Pt(poly) substrate modified by a Cu monolayer, formed during the Cu UPD at +0.35 V. The amount of Cu_{UPD} ranges up to about one equivalent monolayer. These findings are consistent with the general concepts of the formation of a new phase onto a foreign substrate considering a correlation between processes of UPD and OPD of metals in the case of a strong metal-substrate interaction [1, 2, 4, 40].
2. The AFM images suggest at least two morphologically different areas of the Cu_{UPD} layer. This behaviour probably arises from the Cu deposition onto the surface areas with rather low density of defects and onto those with strong inhomogeneities.
3. The presence of H_2SeO_3 in the working solution and, correspondingly, the formation of Se(0) species onto the surface of Pt(poly) electrode [36, 37], manifest themselves mainly in a dual effect. First of all, the Cu UPD is suppressed at higher underpotentials, in particular, at $E > +0.35$ V. Secondly, at lower values of Cu underpotentials, at *E* close to E_r, this process is somewhat enhanced. The coexistence of adsorbed zero valence Cu and Se species was concluded to occur, as established from the XPS measurements. The amount of Se species was found to be no more than a few at. %. From the AFM examination it follows that the addition of H_2SeO_3 to the working solution causes the chain-like structures to be formed on the surface, but the surface roughness characteristics are changed rather slightly.

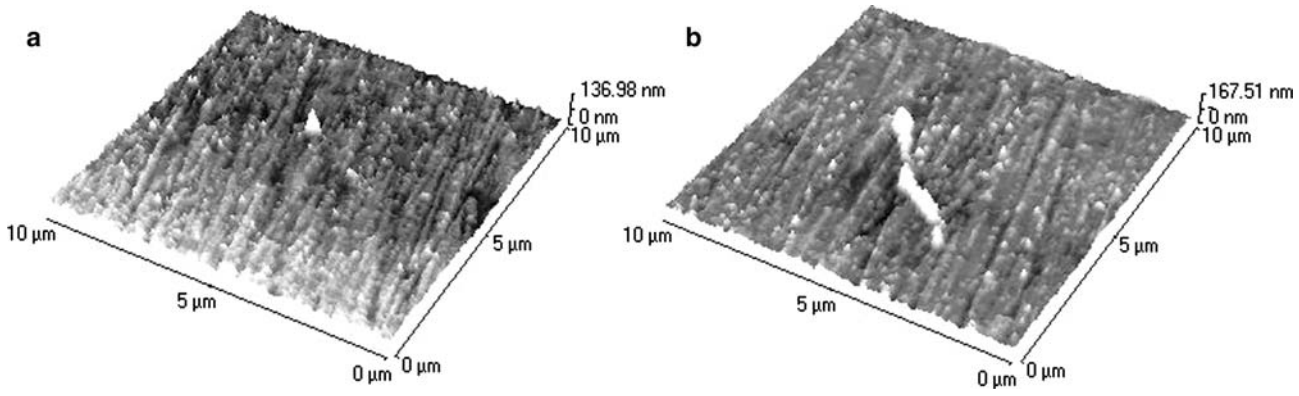

Fig. 4 Ex situ AFM images of a Pt(poly) electrode surface after holding in 0.5 M H_2SO_4 + 0.01 M $CuSO_4$ solution without (**a**) or with 0.005 mM H_2SeO_3 (**b**) at +0.35 V for 2 min

The early stages of Cu deposition in the OPD region

When studying the mechanism and kinetics of nucleation and growth of a new phase onto a foreign substrate, the cyclic voltammetry and potential step techniques are usually applied.

Figure 6 shows a series of typical current transients for the Cu electrodeposition onto Pt(poly) in 0.5 M H_2SO_4 + 0.01 M $CuSO_4$ solution without or with 0.005 mM H_2SeO_3 recorded by applying the potential steps from E_{start} = +0.35 V in the Cu UPD region to different E_{dep} in the Cu OPD region. The transients are characterized by a rising current (I) due to the nucleation and growth of isolated nuclei. As the nuclei grow, the overlap of diffusion fields with localized spherical symmetry gives rise to a current maximum (I_{max}) at t_{max} followed by a decaying current. I_{max} increases and t_{max} decreases as the applied E_{dep} is made more negative. These features are consistent with the Scharifker and Hills (SH) model of 3D nucleation of hemispherical clusters with diffusion-controlled growth [41–43], which has been used extensively for many different systems. This model implies the formation and growth of the initial nuclei onto a surface of foreign substrate at $t < t_{max}$, the overlap of the diffusion zones around them at $t = t_{max}$ and the further growth on an initial layer on a substrate surface at $t < t_{max}$.

The addition of H_2SeO_3 to the working solution was found to result in the decrease in I_{max} and in the increase in t_{max} (Fig. 7).

For the 3D nucleation with diffusion-controlled growth after applying a potential step from a certain value of E_{start} into an overpotential region two limiting cases—instantaneous and progressive nucleation—have been predicted by the SH theory [41–43]. One of the methods for distinguishing between these two limiting case is to compare the experimental transients plotted in a non-dimensional plot, $(I/I_{max})^2$ versus t/t_{max}, with their theoretical plots calculated for instantaneous, Eq. 1, and progressive, Eq. 2, 3D nucleation and growth [43]:

$$\left(\frac{I}{I_{max}}\right)^2 = 1.9542\left(\frac{t}{t_{max}}\right)^{-1}\left\{1-\exp\left[-1.2564\left(\frac{t}{t_{max}}\right)\right]\right\}^2, \quad (1)$$

$$\left(\frac{I}{I_{max}}\right)^2 = 1.2254\left(\frac{t}{t_{max}}\right)^{-1}\left\{1-\exp\left[-2.3367\left(\frac{t}{t_{max}}\right)^2\right]\right\}^2. \quad (2)$$

The experimental $(I/I_{max})^2$ versus (t/t_{max}) plots along with the calculated plots are shown in Fig. 8. The experimental data are presented depending on the absence (Fig. 8a) or the presence of H_2SeO_3 (Fig. 8b). These data show that, within the E_{dep} interval explored, the experimental curves follow closely the response predicted for the instantaneous 3D nucleation with diffusion-controlled growth. Notice that this Cu nucleation mode remains unchanged with adding H_2SeO_3.

Once it is established that the instantaneous 3D nucleation with diffusion-controlled growth model is applicable for the Cu electrodeposition, the number density of formed nuclei (N) at different E_{dep} can be calculated from the values of I_{max} and t_{max} in the chronoamperograms (Figs. 6 and 7) [43]:

$$I_{max} = 0.6382zFDc(k_cN)^{0.5}, \quad (3)$$

$$t_{max} = \frac{1.2564}{N\pi k_e D}, \quad (4)$$

where zF is the molar charge transferred during electrodeposition, D and c are the diffusion coefficient and concentration of metal ions, $k_e = (8\pi\, cM/\rho)^{0.5}$, M and ρ are the molar weight and density of deposited metal. A parameter k_e for Cu is equal to 0.042. According to the accepted SH model [43], the nuclei density N can also be calculated as a function of I_{max} and t_{max} with a more convenient relationship derived from a combination of Eqs. 3 and 4 [44]:

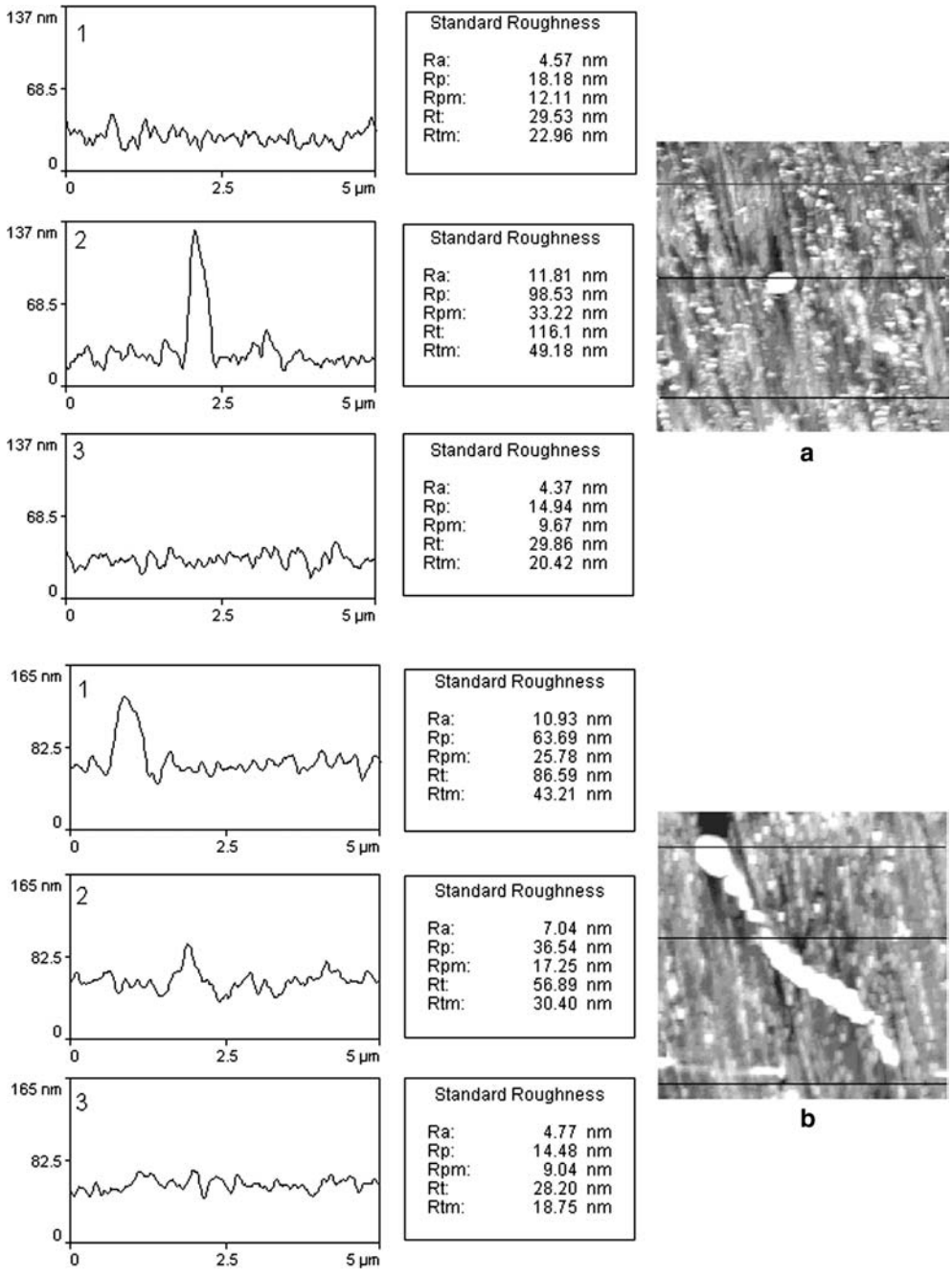

Fig. 5 Cross-sectional profiles along selected lines (from Fig. 4a, b, respectively)

$$N = \frac{0.065(zFc/I_{\max} \cdot t_{\max})^2}{k_e} \quad (5)$$

The size of individual nucleus depends on the deposition time (t_{dep}). Once N is estimated from, say, Eq. 5, and assuming the Cu particles are of spherical shape, an average nucleus radius can be estimated from a charge per unit area of electrode (Q) consumed during deposition using the following relation [45]:

$$r_{av} = \left(\frac{3Qv_m}{4\pi zFN}\right)^{1/3}, \quad (6)$$

where v_m is the molar volume of deposited metal, for Cu $v_m = 7.1$ cm^3 mol^{-1}. Q was evaluated by integrating the corresponding chronoamperograms over the time interval up to $t_{dep} = t_{max}$ assuming that this quantity of charge is mainly due to a faradaic reaction $Cu^{2+} + 2e \rightarrow Cu$. A contribution of parasitic processes such as double layer charging, partial reduction of Cu^{2+} or Se(IV), reduction of Se(0) particles to Se(-II), were considered to be negligible under the given experimental conditions.

When the instantaneous 3D nucleation with diffusion-controlled growth occurs, the diffusion coefficient D

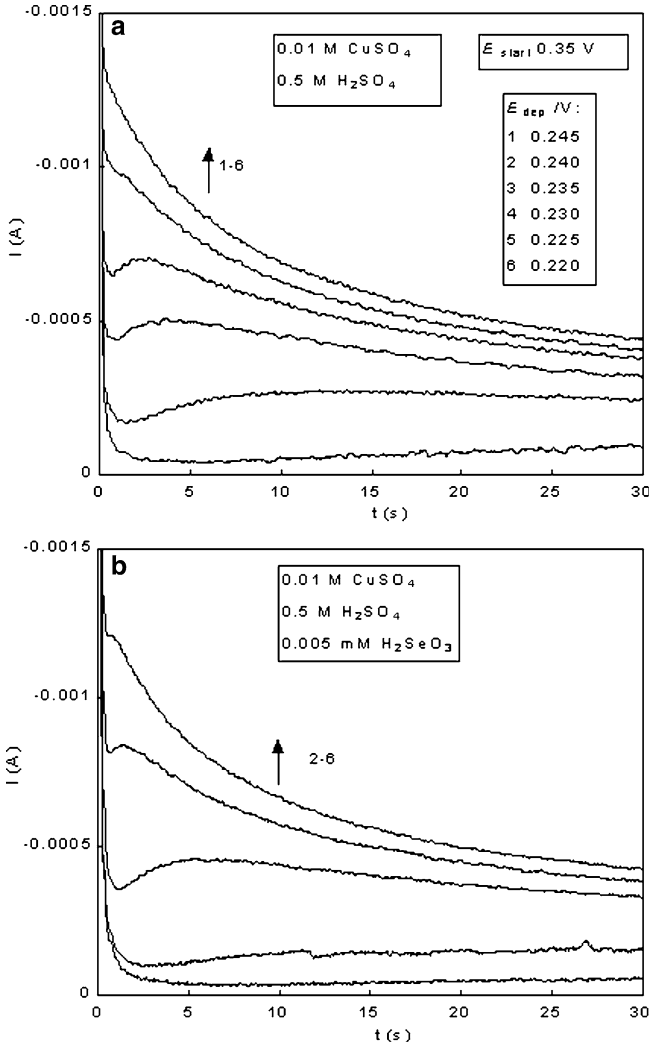

Fig. 6 Typical potentiostatic current transients for the Cu electrodeposition onto the working electrode recorded by E steps from $E_{start} = +0.35$ V to various deposition potential E_{dep} in the Cu OPD region from 0.5 M H_2SO_4 + 0.01 M $CuSO_4$ solution without (**a**) or with 0.005 mM H_2SeO_3 (**b**)

can be re-calculated from a product $I^2_{max}.t_{max}$ according to [43]:

$$I^2_{max} \cdot t_{max} = 0.1629(zFc)^2 D. \quad (7)$$

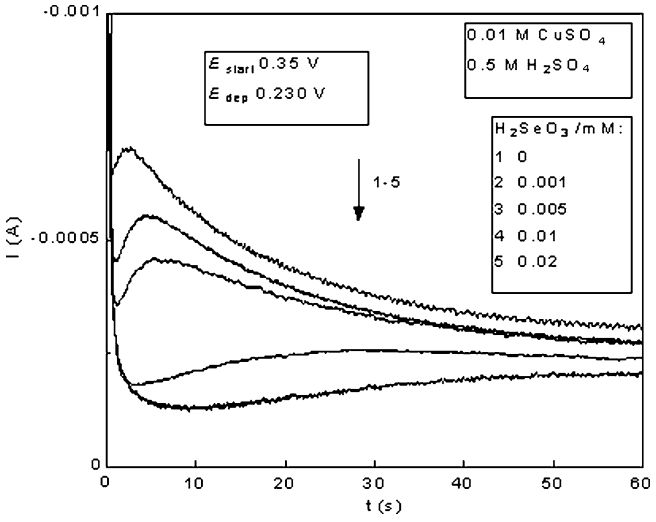

Fig. 7 Potentiostatic current transients for the Cu electrodeposition onto the working electrode recorded by E step from $E_{start} = +0.35$ V and to $E_{dep} = +0.23$ V ($E_{dep} < E_r$) in 0.5 M H_2SO_4 + 0.01 M $CuSO_4$ solution containing different amounts of H_2SeO_3

The calculation yielded $D = 2.9\times10^{-6}$ cm^2 s^{-1} for Cu^{2+} ion in H_2SeO_3-free $CuSO_4$ solution. This value of D is somewhat lower than those reported elsewhere [46]. A similar phenomenon has also been observed recently for other systems, for example, for Zn electrodeposition onto a GC substrate [47]. The reason for this result is not yet clear. It has been pointed out that one of the reasons for such a difference may be a contribution of slow charge transfer or, in other words, the case of the mixed kinetics (diffusion + discharge) instead of a purely diffusion control, as the nucleation occurs at centres of different activity [48].

The calculated values for Cu^{2+}, N and r_{av} are given in Table 1. Data in Table 1 also show that the rather low coverage for the Cu nuclei formation, 10^5 to 10^6 cm^{-2}, was obtained. The calculated density of nuclei corresponds to less than one or about one in 10^9 surface atoms, from the density of atomic sites ($\sim10^{15}$ cm^{-2}) for Pt(poly). Similar results were obtained for other values of E_{dep}. Therefore, it can be concluded that only a small fraction of the total number of Pt(poly) sites is required for the initiation of Cu nucleation and growth. This conclusion agrees well with the results of other authors

Table 1 Numerical values of diffusion coefficient D for Cu^{2+} ion and kinetic parameters of the Cu nucleation and growth—nuclei density N and average nucleus radius r_{av}—obtained from analysis according to the SH model [41–43, 45] of the experimental current transients recorded during the bulk Cu deposition onto Pt(poly) from 0.5 M H_2SO_4 + 0.01 M $CuSO_4$ solution without or with H_2SeO_3. $E_{start} = +0.35$ V, $E_{dep} = +0.23$ V

Concentration of H_2SeO_3 (mM)	$10^4\times I_{max}$ (A cm^{-2})	t_{max} (s)	$10^6\times D$ for Cu^{2+} (cm^2 s^{-1}) from Eq. (7)	$10^{-6}\times N$ (cm^{-2}) from Eq. (5)	r_{av} (μm) from Eq. (6)
0	8.23	2.60	2.91	2.20	0.21
0.001	6.52	4.55		1.15	0.29
0.005	5.30	6.10		0.96	0.31
0.01	3.11	27.65		0.14	0.83

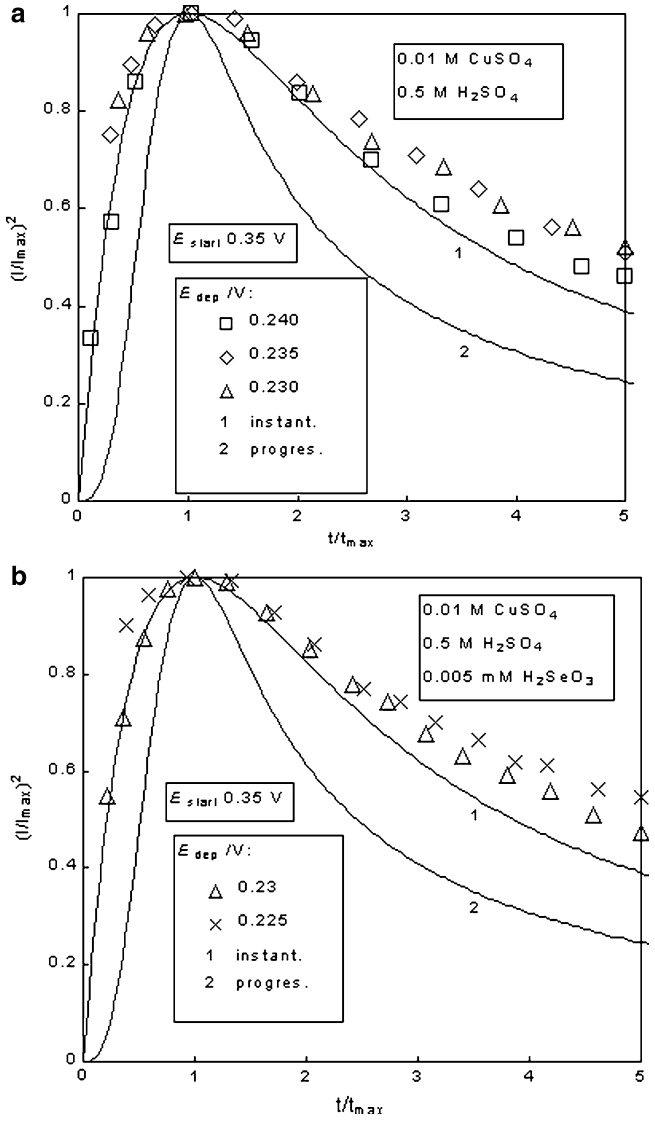

Fig. 8 Dimensionless plots of the potentiostatic current transients recorded in 0.5 M H_2SO_4 + 0.01 M $CuSO_4$ solution without (**a**) or with 0.005 mM H_2SeO_3 (**b**). Lines: theoretical instantaneous (*1*) and progressive (*2*) 3D nucleation and diffusion-controlled growth according to [43]

[7]. As would be expected, N increased with the increase in the Cu overpotential (not shown). The data presented in Table 1 also clearly show the decrease in N and the increase in r_{av} for the Cu nuclei with increasing c of H_2SeO_3.

The morphology of Cu deposited onto the Pt(poly) electrode was further examined by ex situ AFM. In all the cases Cu was deposited by a single E step from $E_{start} = +0.35$ V to $E_{dep} = +0.23$ V. The electrolysis was terminated after 10 or 30 s corresponding to the values of t/t_{max} of 3.85 and 11.5. The total charges Q calculated from the corresponding current transients were found to be about 6.6 or 15.5 mC in the absence of H_2SeO_3 and about 4.8 or 12.3 mC in the presence of 0.005 mM H_2SeO_3. It can be suggested from these values of Q, that the amount of deposited Cu corresponded to about 8 or 20 and 6 or 16 equivalent monolayers, respectively. Different regions of the electrode surface were imaged, but only image is presented for every case.

After the electrodeposition of Cu from the working solution without H_3SeO_3 for 10 s, it was found that the AFM image was relatively similar to that observed from the Cu-precovered Pt(poly) electrode (Fig. 4a), that is, morphological features associated with the 3D nucleation and growth process were not clearly revealed. With the application of a prolonged deposition time (30 s), the morphological changes which could be attributed to the 3D nucleation and growth process are revealed (Fig. 9a). The individual clusters were found to be of comparable sizes and randomly distributed on the surface with a density of about 9×10^8 cm^{-2}. As one can see, in the local regions of the surface some kind of rather large agglomerates composed of the clusters of different diameter are also observed. Such protrusions appear to be associated with the Cu UPD (Fig. 4a). Once again this emphasizes the influence of surface imperfections on the course of electrocrystallization process. Cu deposit tended to be formed along the polishing scratches indicating that these scratches acted as active sites for the deposition process.

Close inspection of the AFM image at higher magnification from the region surrounding the agglomerates mentioned above (Fig. 9c) revealed that the Cu clusters still did not completely coalesce at the values of E_{dep} and t_{dep} applied.

Figure 10 shows a cross-sectional profile of the surface along a line as shown in a top-view image. From this profile a lateral distance and height can be determined. It was found that a ratio between the growth in the lateral direction and that in the vertical direction was more or less the same as in the case of the Cu UPD. From the standard roughness measurements, it was obtained that the arithmetic roughness average, R_a, was about 7.8 nm and the maximum height of the profile above a mean line, R_p, was about 22.3 nm.

In the solution containing H_2SeO_3, the presence of distinct chain-like structures (Fig. 9b) somewhat resembles the surface morphology of the Cu-precovered Pt(poly) electrode (Fig. 4). These structures were found to be composed of numerous separate particles. In the zones around them, the rather homogeneous distribution of elongated clusters and separate particles can be revealed (Fig. 9d) with a density of about 6×10^9 cm^{-2} (Fig. 11).

Consequently, the values of N obtained by AFM imaging were found to be about two orders larger than those from the chronoamperometric measurements (Table 1). Such discrepancies between the nuclei densities (visual counting on structural images) and the values of N obtained from the analysis of chronoamperometric data have already been reported for various systems, for example, Pb onto GC [48] and onto *n*-Ge(111) [49], Hg onto vitreous carbon [50], Cu onto TiN [51] and onto GC [52], Au onto *n*-Si(100) [53], etc. The reason for the significant discrepancies between the measured nuclei densities and those estimated from the potentiostatic

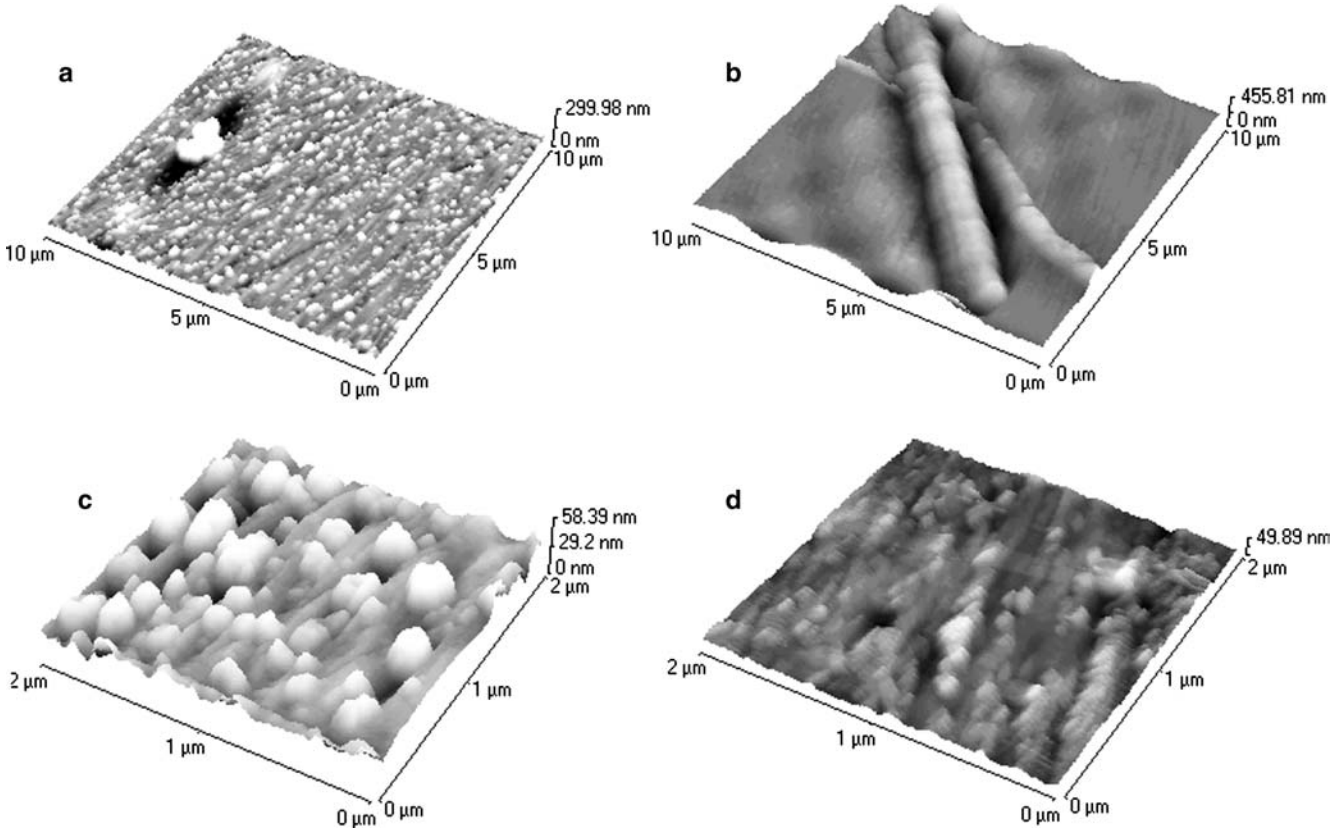

Fig. 9 Ex situ AFM images of Pt(poly) surface after the Cu electrodeposition by E step from $E_{start} = +0.35$ V to $E_{dep} = +0.23$ V for $t_{dep} = 30$ s from 0.5 M H_2SO_4 + 0.01 M $CuSO_4$ solution without (**a**, **c**) or with 0.005 mM H_2SeO_3 (**b**, **d**). Images (**c**) and (**d**) at higher magnification of the local surface regions surrounding the large agglomerates shown in (**a**) and (**b**), respectively

current transients has been pointed out to be not clear [51–53]. A possible explanation, among others, is that I_{max} and t_{max} do not accurately describe the time of overlap of the diffusion zones of individual growing nuclei and, hence, the formation of multiple nuclei instead of an individual nucleus within a single diffusion

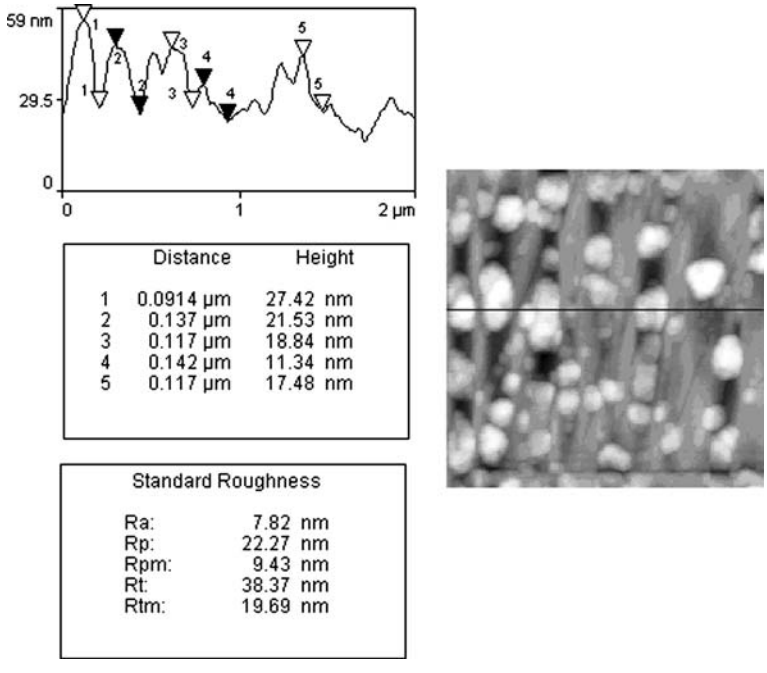

Fig. 10 Cross-sectional profile along a selected line (from Fig. 4a, c)

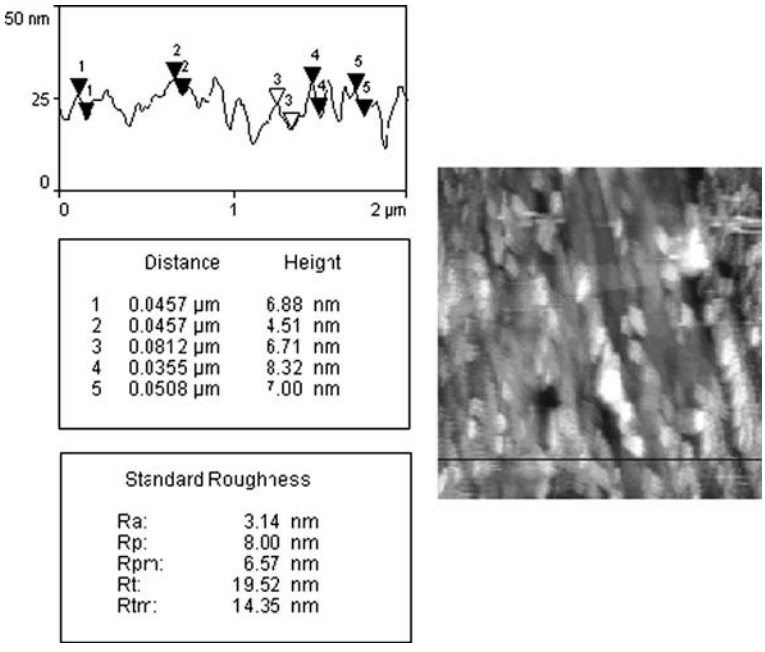

Fig. 11 Cross-sectional profile along a selected line (from Fig. 4b, d)

zone becomes possible [50, 51, 53]. Such a discrepancy may also be connected with a mixed, rather than purely diffusion, control over the crystal growth [52]. Although the estimation of N by a visual counting using *ex situ* methods somewhat suffers from uncertainties depending on samples handling or a sensitivity of a method applied, it seems that, in the case under study, such a way for the calculation of N should better describe the system.

The growth of Cu clusters and particles was found to be favoured in the x-y directions rather than in the z-direction, especially in the presence of H_2SeO_3, when the ratio x/z increased by about 24% (Figs. 10 and 11). In solution with this additive, the parameters R_a and R_p were obtained to be of less magnitudes, namely, about 3.1 and 8.0 nm, respectively, suggesting a rather strong smoothening effect of H_2SeO_3.

It was also found that the actual charge consumed during the Cu deposition (Fig. 9) should be of 23 and 58.7 mC in the absence and in the presence of H_2SeO_3, respectively. This calculation was performed assuming the hemispherical shape of Cu particles. These values of Q are markedly larger than those obtained from the chronoamperometric measurements. Such a discrepancy between the values of Q calculated from the chronoamperometric and AFM results may be explained by the fact that the Cu nuclei are not hemispherically shaped, as, indeed, followed from the ratio x/z. In addition, this discrepancy may also be associated to some extent with difficulties in determining the true lateral dimensions of the Cu nuclei (Figs. 10 and 11).

Conclusions

The analysis of the electrochemical data points to the instantaneous 3D nucleation and diffusion-controlled growth of formed Cu nuclei model proposed by SH for the early stages of Cu electrodeposition from an acidic $CuSO_4$ solution without or with an additive H_2SeO_3 onto a Pt(poly) surface precovered independently with underpotentially deposited Cu. The values of diffusion coefficient D for Cu^{2+} ion, number of nuclei N being of the order of 10^6 to 10^7 cm^{-2}, a rather low value, and average nucleus radius r_{av} were evaluated from the chronoamperometric data. The parameters of the electrocrystallization were dependent on the deposition potential E_{dep} and the amount of H_2SeO_3 in the working solution. The addition of H_2SeO_3 was shown to decrease N and to increase r_{av}.

The AFM imaging revealed that the Cu clusters were of comparable and rather homogeneously distributed on the Pt(poly) electrode surface with a density of about 9×10^8 cm^{-2} in the absence of H_2SeO_3 and 6×10^9 cm^{-2} in the presence of this additive in amount of 0.005 mM. In the local regions of the surface rather large agglomerates composed of the different diameter particles were also observed in both cases, but in the solution with H_2SeO_3 these agglomerates were of a chain-like configuration. The growth of formed Cu clusters was found to be favoured in the x-y directions rather than in the z-direction, especially in the presence of H_2SeO_3. The possible reasons for the discrepancies which were observed between certain findings from the chronoamperometric measurements and those from the AFM imaging were discussed.

References

1. Budevski E, Staikov G, Lorenz WJ (2000) Electrochim Acta 45:2559
2. Lorenz WJ, Staikov G, Schindler W, Wiesbeck W (2002) J Electrochem Soc 149:K47

3. Martins ME, Salvarezza RC, Arvia AJ (1992) Electrochim Acta 37:2203
4. Kolb DM (1978) Physical and electrochemical properties of metal monolayers on metallic substrates. In: Gerischer H, Tobias ChW (eds) Advances in electrochemistry and electrochemical engineering, vol 11. Wiley, New York, pp 125–271
5. Furuya N, Motoo S (1976) J Electroanal Chem 72:165
6. Hammond JS, Winograd N (1977) J Electroanal Chem 80:123
7. Margheritis D, Salvarezza RC, Giordano MC, Arvia AJ (1987) J Electroanal Chem 229:327
8. Plieth W (1992) Electrochim Acta 37:2115
9. Nichols RJ, Beckmann W, Meyer H, Batina N, Kolb DM (1992) J Electroanal Chem 330:381
10. Michailova E, Vitanova I, Stoychev D, Milchev A (1993) Electrochim Acta 38:2455
11. Fabricius G, Kontturi K, Sundholm G (1994) Electrochim Acta 39:2353
12. Rynders RM, Alkire RC (1994) J Electrochem Soc 141:1166
13. Peykova M, Michailova E, Stoychev D, Milchev A (1995) Electrochim Acta 40:2595
14. Rashkov R, Nanev C (1995) J Appl Electrochem 25:603
15. Hölzle MH, Apsel CW, Will T, Kolb DM (1995) J Electrochem Soc 142:3741
16. Tarallo A, Heerman L (1999) J Appl Electrochem 29:585
17. Radisic A, West AC, Searson PC (2002) J Electrochem Soc 149:C94
18. Llorca MJ, Herrero E, Feliu JM, Aldaz A (1994) J Electroanal Chem 373:217
19. Herrero E, Rodes A, Pérez JM, Feliu JM, Aldaz A (1996) J Electroanal Chem 412:165
20. Bhattacharya RN, Fernandez AM, Contreras MA, Keane J, Tenant A, Ramanathan K, Tuttle JR, Noufi RN, Hermann AM (1996) J Electrochem Soc 143:854
21. Lippkow D, Strehblow H-H (1998) Electrochim Acta 43:2131
22. Carbonnelle P, Lamberts L (1992) J Electroanal Chem 340: 53
23. Massaccesi S, Sanchez S, Vedel J (1993) J Electrochem Soc 140:2540
24. Marlot A, Vedel J (1999) J Electrochem Soc 146:177
25. Kemell M, Saloniemi H, Ritala M, Leskelä M (2000) Electrochim Acta 45:3737
26. Hill MRH, Rogers GT (1976) J Electroanal Chem 68:149
27. Lezhava TI (1989) Acceleration at Metal Deposition. Diss Frumkin Inst Electrochem, Moscow
28. Steponavičius A, Šimkūnaitė D, Jasulaitienė V (1997) Chemija No 2:64
29. Riveros G, Henriquez R, Córdova R, Schrebler R, Dalchiele EA, Gómez H (2001) J Electroanal Chem 504:160
30. Steponavičius A, Šimkūnaitė D, Lichušina S, Kapočius V (2001) Chemija 12:147
31. Steponavičius A, Šimkūnaitė D (2002) Bull Electrochem 18:367
32. Biegler T, Rand DAJ, Woods R (1971) J Electroanal Chem 29:269
33. Steponavičius A, Šimkūnaitė D (2002) Rus J Electrochem 38:488
34. Jerkiewicz G, Vatankhab Gh, Lessard J, Soriaga MP, Park Y-S (2004) Electrochim Acta 49:1451
35. Danilov AI, Molodkina EB, Polukarov YuM (2000) Rus J Electrochem 36:976
36. Šimkūnaitė D, Ivaškevič E, Jasulaitienė V, Steponavičius A (2003) Bull Electrochem 19:437
37. Šimkūnaitė D, Ivaškevič E, Jasulaitienė V, Kaliničenko A, Valsiūnas I, Steponavičius A (2004) Chemija 15:12
38. Bosco E, Rangarajan SK (1981) J Chem Soc Faraday Trans 1 77:1673
39. Breiter MW (1969) Trans Faraday Soc 65:2197
40. Jüttner K, Lorenz WJ, Staikov G, Budevski E (1978) Electrochim Acta 23:741
41. Gunawardena GA, Hills GJ, Montenegro I (1978) Electrochim Acta 23:693
42. Gunawardena GA, Hills G, Montenegro I, Scharifker B (1982) J Electroanal Chem 138:225
43. Scharifker B, Hills G (1983) Electrochim Acta 28:879
44. Grujicic D, Pesic B (2002) Electrochim Acta 47:2901
45. Leone A, Marino W, Scharifker BR (1992) J Electrochem Soc 139:438
46. Quickenden TI, Xu Q (1996) J Electrochem Soc 143:1248
47. Yu J, Wang L, Su L, Ai X, Yang H (2003) J Electrochem Soc 150:C19
48. Palmisano F, Desimoni E, Sabbatini L, Torsi G (1979) J Appl Electrochem 9:517
49. Ehlers C, König U, Staikov G, Schultze JW (2001) Electrochim Acta 47:379
50. Serruya A, Mostany J, Scharifker BR (1999) J Electroanal Chem 464:39
51. Radisic A, Long JG, Hoffmann PM, Searson PC (2001) J Electrochem Soc 148:C41
52. Danilov AI, Molodkina EB, Baitov AA, Pobelov IV, Polukarov YuM (2002) Rus J Electrochem 38:743
53. Oskam G, Searson PC (2000) J Electrochem Soc 147:2199